Half-collision model for multiple ionization by photon impact

Thomas Pattard[1,*] and Joachim Burgdörfer[1,2]
[1]*Department of Physics and Astronomy, University of Tennessee, Knoxville, Tennessee 37996-1200*
[2]*Institute for Theoretical Physics, Vienna University of Technology, A1040 Vienna, Austria*
(Received 13 March 2001; published 18 September 2001)

We present a simple half-collision model that allows the approximate calculation of absolute cross sections for multiple ionization by breaking this process down into a primary ionization event followed by a half-scattering event in which additional electrons are ionized. As a critical test for the feasability of this approach, we consider the double ionization of two-electron systems, which we describe in terms of the single ionization of the ''primary'' electron followed by impact ionization of the slow ''secondary'' electron. For triple ionization of lithium, the model decomposes the three-electron breakup process into a double ionization of the two inner electrons followed by electron-electron half-scattering of the receding electrons at the residual ''spectator'' $2s$ electron. We find surprisingly good agreement with recent experimental data.

DOI: 10.1103/PhysRevA.64.042720 PACS number(s): 32.80.Fb, 34.80.Kw, 34.90.+q

I. INTRODUCTION

In recent years, considerable progress has been made in the understanding and theoretical description of multiple excitation and ionization processes induced by single-photon absorption. Experimental and theoretical activities have focused primarily on two-electron emission. Accurate measurements of double ionization, in particular the ratio of double to single ionization, have become available [1,2]. At the same time, accurate *ab initio* methods have been developed that allow for a quantitative description of two-electron processes such as double ionization or ionization and excitation [3–7]. The methods currently employed heavily rely on large-scale numerical calculations that push the limit of existing computing resources. Going beyond two active electrons within an *ab initio* calculation, treating correlations between all electrons, still appears to be beyond the present computational capabilities. Meanwhile, pioneering experiments on the triple photoionization of lithium have been reported [8,9]. Theoretical efforts initially focused on the asymptotic limit of high photon energies $E_{\mathrm{ph}}\rightarrow\infty$ for which predictions can be made within the framework of ''shake'' approximations [10,11]. For finite photon energies, no *ab initio* calculation is, to our knowledge, available.

In this paper, we present an analysis of multiple ionization based on a half-collision model (HCM). A preliminary description of the model and its application to the lithium triple ionization has already been reported previously [12]. Here, we give a detailed account of the model. Moreover, by application to the double ionization case, which can be treated *ab initio*, we give a critical analysis of its limitations and range of applicability. The HCM can be considered as an extension of a simple picture originally suggested by Samson [13] for double ionization: the ejection of the second electron should resemble electron impact ionization by the primary electron that absorbs the photon and leaves the atom at a high speed. Consequently, the ratio of double to single ionization at high photon energies, which is proportional to the conditional probability for ejection of the second electron upon photon absorption by the first electron, should be proportional to the electron-impact ionization cross section of the singly charged ion. By allowing for electron-electron scattering, electron correlation effects in the double continuum can be approximately taken into account. There are, however, important differences to electron-impact ionization; as the primary electron absorbing the photon (the projectile) is initially localized inside the atom near the nucleus, the electron-electron interaction ''on the way out'' corresponds to a ''half-collision.'' This process, which can be associated with certain diagrams within the framework of many-body perturbation theory (see, e.g., Ref. [14]), is sometimes referred to as ''TS1.'' Moreover, while the electron-impact ionization cross section decreases $\propto 1/E$ (or $\ln E/E$ for dipole allowed transitions) with the energy of the ionizing particle, the double-ionization cross section should converge to the ''shake-off'' limit as $E=E_{\mathrm{ph}}\rightarrow\infty$ rather than to zero as in the original model [13].

In this paper we present the application of the HCM to two processes, the double ionization of helium and the triple ionization of lithium. Within the HCM for the double ionization, this process is decomposed into the photon absorption (i.e., single ionization) and the subsequent electron-electron interaction of an electron-impact ionization, where the two parts can be calculated separately. As we will show below, for intermediate to high energies, the HCM yields good agreement with fully *ab initio* calculations for the double ionization of helium. For triple ionization, we decompose this process into double ionization of the two deeply bound, strongly correlated $1s$ electrons followed by half-collisions of the two receding electrons with the third, weakly bound $2s$ electron. This decomposition exploits the strong nonequivalence of the inner and outer electrons on Li-like systems. The binding energy of the two inner electrons $E_B(1s^2)$ accounts for $\approx 97\%$ of the total binding energy. The intershell correlation between the inner and outer electron is very weak and the electronic wave functions are spatially well

*Present address: MPI for the Physics of Complex Systems, Nöthnitzer Strasse 38, D-01187 Dresden, Germany

separated due to the large difference in radii, $\langle r\rangle_{1s}/\langle r\rangle_{2s} \ll 1$. The primary photon absorption at high energies will therefore take place in the $1s$ shell, which suggests the double ionization of the $1s^2$ pair as the dominant precursor to triple ionization. With this ansatz, we find remarkably good agreement with recent data considering the simplicity of the model.

The paper is organized as follows: In Sec. II, we will introduce the half-collision model and present applications for the case of double ionization. We will show that the corresponding equations can be derived from a Born-type perturbation expansion and present numerical benchmark calculations for helium. The results are compared with data from highly accurate *ab initio* methods. After establishing the usefulness of the HCM in the two-electron case, we will show in Sec. III the generalization to triple ionization. The paper ends with a brief summary and a short outlook (Sec. IV). In order not to divert the reader from the basic ideas of the approach, a few of the technical details are given in the Appendices. Atomic units are used throughout the paper unless otherwise stated.

II. THE HALF-COLLISION MODEL FOR DOUBLE PHOTOIONIZATION

In this section we will derive the equations underlying the HCM from a perturbation expansion and apply the model to the double photoionization of helium. The resulting expressions can be evaluated numerically and the results for helium are compared with well-known accurate *ab initio* methods. Helium serves as a test case for two reasons: For one, the two-electron problem can be accurately treated with current computational capabilities and can therefore serve as a gauge for semiempirical models. Furthermore, for the HCM, which treats the emission of the ''primary'' and the ''scattered'' electron on an unequal footing, the two-electron emission from the symmetric helium ($1s^2$) ground state is the ''worst-case'' scenario and therefore provides a stringent test.

A. Notation

We denote the initial and final state by

$$|\Psi_i\rangle = |\psi_i(1,2)\rangle |n_{\omega,\sigma}=1\rangle \tag{1}$$

and

$$|\Psi_f\rangle = |\phi_f(1)\phi_{\mathbf{k}_f}(2)\rangle |n_{\omega,\sigma}=0\rangle, \tag{2}$$

where $n_{\omega,\sigma}$ is the occupation number of mode ω and polarization σ of the photon field, and we assume that the final state contains at least one electron in the continuum with wave number $\mathbf{k}_f$. For reasons of technical simplicity, we will later assume that k_f is large enough that this electron can be described by a plane wave $|\mathbf{k}_f\rangle$. The latter assumption is, however, not an essential ingredient to the model. Such an approximation for the final state is justified only for high photon energies, but we will show below that it nevertheless leads to surprisingly good results over a wide energy range. We write the model Hamiltonian underlying the HCM as

$$H = h(1) + h(2) + h_{ph} + V_{ee}^{(1,2)} + W^{(2,ph)} \tag{3}$$

where $V_{ee}^{(1,2)} = 1/|\mathbf{r}_1 - \mathbf{r}_2|$ describes the electron-electron interaction and $W = (1/c)\mathbf{p}_2 \cdot \mathbf{A}$ the interaction between the electromagnetic field and the atom. For simplicity, we treat here and in the following the primary and secondary electron, i.e., the ionizing and ionized electron, in the half-scattering process as distinguishable. Clearly, a complete description requires proper antisymmetrization. We furthermore define the channel Hamiltonians H^α and H^β as

$$H^\alpha = h(1) + h(2) + h_{ph} + V_{ee}^{(1,2)}, \tag{4}$$

$$H^\beta = h(1) + h(2) + h_{ph}, \tag{5}$$

with channel perturbations

$$V^\alpha = H - H^\alpha = \frac{1}{c}\mathbf{p}_2 \cdot \mathbf{A} \tag{6}$$

and

$$V^\beta = H - H^\beta = V_{ee}^{(1,2)} + W^{(2,ph)} \equiv V_{ee} + \frac{1}{c}\mathbf{p}_2 \cdot \mathbf{A}. \tag{7}$$

Accordingly, $|\Psi_i\rangle$ is an eigenstate of H^α

$$H^\alpha |\Psi_i\rangle = (E_i + e_i)|\Psi_i\rangle = E_i^{tot}|\Psi_i\rangle \tag{8}$$

and $|\Psi_f\rangle$ is one of H^β

$$H^\beta |\Psi_f\rangle = (\epsilon_f + k_f^2/2 + e_f)|\Psi_f\rangle = E_f^{tot}|\Psi_f\rangle. \tag{9}$$

In the above equations, e stands for the energy of the photon field, E_i is the energy of the atom in the ground state, and ϵ and $k^2/2$ are the energies associated with electrons 1 and 2, respectively, in the final state. Finally, the energy of the singly occupied photon mode is

$$\omega_{ph} = e_i - e_f. \tag{10}$$

B. Born series for the transition amplitude

We are interested in the transition amplitude

$$a_{fi} = \langle \Psi_f | S | \Psi_i \rangle, \tag{11}$$

where the S matrix is defined as (e.g., [15])

$$S = \lim_{T\to\infty\, T'\to-\infty} e^{iH^\beta T} U(T,T') e^{-iH^\alpha T'}. \tag{12}$$

Standard multichannel scattering theory leads to a series expansion for the transition amplitude (Appendix A), which reads

$$a_{fi}=\lim_{T\to\infty T'\to-\infty}\langle\phi_f(1)\phi_{\mathbf{k}_f}(2)n_{\omega,\sigma}=0|e^{iH^\beta T}e^{-iH^\alpha T}|\psi_i(1,2)n_{\omega,\sigma}=1\rangle$$
$$+\left\langle\phi_f(1)\phi_{\mathbf{k}_f}(2)n_{\omega,\sigma}=0\left|-i\int_{T'}^{T}dt_1e^{iH^\beta t_1}V^\alpha e^{-iH^\alpha t_1}\right|\psi_i(1,2)n_{\omega,\sigma}=1\right\rangle$$
$$+\left\langle\phi_f(1)\phi_{\mathbf{k}_f}(2)n_{\omega,\sigma}=0\left|(-i)^2\int_{T'}^{T}dt_1\int_{t_1}^{T}dt_2e^{iH^\beta t_2}V^\beta e^{-iH^\beta t_2}e^{iH^\beta t_1}V^\alpha e^{-iH^\alpha t_1}\right|\psi_i(1,2)n_{\omega,\sigma}=1\right\rangle+\cdots. \tag{13}$$

Because of the orthogonality of the Fock states,

$$\langle n_{\omega,\sigma}=0|n_{\omega,\sigma}=1\rangle=0, \tag{14}$$

the first nonvanishing contribution to a_{fi} originates from the second term in Eq. (13),

$$a_{fi}^I=-i\int_{T'}^{T}dt_1e^{i(E_f^{tot}-E_i^{tot})t_1}\langle\phi_f(1)\phi_{\mathbf{k}_f}(2)n_{\omega,\sigma}=0|\frac{1}{c}\mathbf{p}_2\cdot\mathbf{A}|\psi_i(1,2)n_{\omega,\sigma}=1\rangle. \tag{15}$$

Taking the limit $T\to\infty$, $T'\to-\infty$, the first-order term for the transition amplitude becomes

$$a_{fi}^I=-i\int_{-\infty}^{\infty}dt_1e^{i(E_f^{tot}-E_i^{tot})t_1}\langle\phi_f(1)\phi_{\mathbf{k}_f}(2)n_{\omega,\sigma}=0|\frac{1}{c}\mathbf{p}_2\cdot\mathbf{A}|\psi_i(1,2)n_{\omega,\sigma}=1\rangle$$
$$=-i\,2\pi\,\delta(E_f-E_i-\omega_{ph})\langle\phi_f(1)\phi_{\mathbf{k}_f}(2)n_{\omega,\sigma}=0|\frac{1}{c}\mathbf{p}_2\cdot\mathbf{A}|\psi_i(1,2)n_{\omega,\sigma}=1\rangle. \tag{16}$$

The physical picture is that of an atom in a (ground) state with energy E_i absorbing a photon with energy ω, which leads to ionization of electron 2 and simultaneously to excitation of electron 1 to a (bound or continuum) state ϕ_f in a ''shake'' process. This results in the well known ''shake limit'' which provides the correct (nonrelativistic) high photon energy limit for multiple ionization. The second-order contribution originating from the third term in Eq. (13) is

$$a_{fi}^{II}=-\sum\!\!\!\!\!\!\int_{a,b}\int_{T'}^{T}dt_1\int_{t_1}^{T}dt_2e^{i(E_f^{tot}t_2-E_i^{tot}t_1)}\langle\phi_f(1)\phi_{\mathbf{k}_f}(2)n_{\omega,\sigma}=0|V_{ee}e^{-iH^\beta t_2}|\psi_{ab}\rangle\langle\psi_{ab}|e^{iH^\beta t_1}\frac{1}{c}\mathbf{p}_2\cdot\mathbf{A}|\psi_i(1,2)n_{\omega,\sigma}=1\rangle. \tag{17}$$

The physical picture underlying Eq. (17) is that of an atom absorbing a photon, creating an intermediate state ψ_{ab} in the process which, in turn, leads to a final state by electron-electron scattering. Choosing as basis states ψ_{ab} the eigenstates of H^β, we find

$$a_{fi}^{II}=-2\pi\,\delta(E_f-E_i-\omega_{ph})\sum\!\!\!\!\!\!\int_{a,b}\int_{0}^{\infty}dte^{i(E_f-E_{ab})t}\langle\phi_f(1)\phi_{\mathbf{k}_f}(2)|V_{ee}|\psi_{ab}(1,2)\rangle\langle\psi_{ab}(1,2)n_{\omega,\sigma}=0|\frac{1}{c}\mathbf{p}_2\cdot\mathbf{A}|\psi_i(1,2)n_{\omega,\sigma}=1\rangle. \tag{18}$$

The final-state electron-electron correlation is taken into account in Eq. (18) to first order of V_{ee} while the amplitude a_{fi}^{II} is, overall, of second order. From the derivation of the series expansion (Appendix A), it is easy to see that the higher-order terms in the expansion correspond to contributions that are to first order in the photon-atom interaction and to subsequently higher orders in V_{ee}. This is analogous to the so-called strong potential Born theory familiar from charge-exchange calculations in ion-atom scattering [16,17]. In our case, the ''weak'' potential, taken to first order, is the photon-atom interaction, while the Coulomb interaction can be taken into account to arbitrary order. The obvious generalization to infinite order in V_{ee} would then be to replace V_{ee} in Eq. (18) by the Coulomb T matrix for electron-electron scattering

$$a_{fi}^{II}=-2\pi\,\delta(E_f-E_i-\omega)\sum\!\!\!\!\!\!\int_{a,b}\int_{0}^{\infty}dte^{i(E_f-E_{ab})t}\langle\phi_f(1)\phi_{\mathbf{k}_f}(2)|T_{ee}|\psi_{ab}(1,2)\rangle\langle\psi_{ab}(1,2)n_{\omega,\sigma}=0|\frac{1}{c}\mathbf{p}_2\cdot\mathbf{A}|\psi_i(1,2)n_{\omega,\sigma}=1\rangle. \tag{19}$$

For later reference, we note that in the generalized form, Eq. (19), the range of the HCM could be extended to lower photon energies, i.e., to lower kinetic energies of the ejected primary electron. We restrict ourselves in the following to the numerical evaluation of the lowest-order perturbation theory. Combining Eqs. (18) and (16) yields

$$a_{fi}=-2\pi i\,\delta(E_f-E_i-\omega_{ph})\sum\!\!\!\!\!\!\int_{a,b}\langle\psi_{ab}(1,2)n_{\omega,\sigma}=0|\frac{1}{c}\mathbf{p}_2\cdot\mathbf{A}|\psi_i(1,2)n_{\omega,\sigma}=1\rangle\Big(\langle\phi_f(1)\phi_{\mathbf{k}_f}(2)|\psi_{ab}(1,2)\rangle$$
$$-i\int_0^\infty dt\,e^{i(E_f-E_{ab})t}\langle\phi_f(1)\phi_{\mathbf{k}_f}(2)|V_{ee}|\psi_{ab}(1,2)\rangle\Big). \tag{20}$$

At very high photon energies, the first-order contribution in Eq. (20) leads to the asymptotic shake factor [18]

$$\langle\phi_f(1)\phi_{\mathbf{k}_f}(2)n_{\omega,\sigma}=0|\frac{1}{c}\mathbf{p}_2\cdot\mathbf{A}|\psi_i(1,2)n_{\omega,\sigma}=1\rangle$$
$$\to\left(\frac{2\pi}{L}\right)^{3/2}4\sqrt{2}\,Z\times\cos(\gamma)\,k_f^{-4}\langle\phi_f(1)|\psi_i(1,\mathbf{r}_2=0)\rangle. \tag{21}$$

Here, γ is the angle between $\mathbf{k}_f$ and the photon polarization vector, and the factor $(2\pi/L)^{3/2}$ stems from the box quantization of the photon field. We now employ a straight-line impact-parameter approximation (see Appendix B for details) for the fast electron taking off near the nucleus (''half-scattering''). The transition amplitude is then given to second order by

$$a_{fi}=-2\pi i\,\delta(E_f-E_i-\omega_{ph})\left(\frac{2\pi}{L}\right)^{3/2}4\sqrt{2}\,Z\cos(\gamma)\frac{1}{(2E_f)^2}$$
$$\times\Big(\langle\phi_f|\psi_i(1,\mathbf{r}_2=0)\rangle-i\sum\!\!\!\!\!\!\int_a\int_0^\infty dt\langle\phi_f|V_{ee}(t)|\phi_a\rangle$$
$$\times e^{i(\epsilon_f-\epsilon_a)t}\langle\phi_a|\psi_i(1,\mathbf{r}_2=0)\rangle\Big). \tag{22}$$

In Eq. (18), we chose the intermediate states ψ_{ab} to be eigenstates of H^β. They are therefore products $\phi_a(\mathbf{r}_1)\phi_b(\mathbf{r}_2)$ of one-electron hydrogenic states. From the doubly infinite sum over these intermediate states, one sum is removed by the impact-parameter approximation, but a summation over a complete set of single-particle states ϕ_a is still required. In addition to the impact-parameter approximation described in detail in the appendices, we made the approximation (which is implicit in any impact-parameter treatment) that the energy transfer during the half-collision is small and the secondary electron will be slow so that $k_f^2/2\approx E_f$. For a numerical evaluation, expression (22) is still not well suited because of the infinite sum over intermediate states and the highly oscillatory nature of the integrals. However, with one further approximation one can greatly reduce the numerical effort. In our calculations, the energy ϵ_a of the intermediate state was replaced by an average energy $\langle\epsilon\rangle$ independent of ϕ_a, thereby invoking a closure approximation. In this case, the transition amplitude is reduced to

$$a_{fi}=-2\pi i\,\delta(E_f-E_i-\omega_{ph})$$
$$\times\left(\frac{2\pi}{L}\right)^{3/2}4\sqrt{2}\,Z\cos(\gamma)\frac{1}{(2E_f)^2}\Big(\langle\phi_f|\psi_i(1,\mathbf{r}_2=0)\rangle$$
$$-i\int_0^\infty dt\langle\phi_f|V_{ee}(t)e^{i(\epsilon_f-\langle\epsilon\rangle)t}|\psi_i(1,\mathbf{r}_2=0)\rangle\Big). \tag{23}$$

Finally, the probabilities for single and double ionization are obtained by summing over bound and integrating over continuum states, respectively, of the secondary electron. Note that all prefactors as well as density-of-states for the photon field and for the primary electron (i.e., the photoabsorption probability) drop out when calculating the ratio σ^{2+}/σ^{+}.

At this point, it may be worthwhile to point out a few differences and similarities to the case of double ionization by charged particles [19]. The analogous process [Eq. (22)] is in this case referred to as ''TS1'' (where 1 refers to first-order perturbation in both electron-electron scattering and primary ionization) and closely resembles the half-scattering process. The major differences lie in the primary ionization event. Charged-particle ionization is not confined to near-zero impact parameter but extends over the entire atomic charge cloud. The matrix element is not restricted to $\mathbf{r}_2=0$. The ejected primary electron spectrum is broad with a peak at near-zero energy rather than δ shaped for photoelectrons. This has profound consequences for the ratio σ^{2+}/σ^{+} [20]. Moreover, the final state is a four-body rather than a three-body Coulomb continuum state. The exit channel perturbation due to the receding projectile (proton, electron) cannot be neglected unless asymptotic speeds ($v_P>10$ a.u.) are reached.

C. Numerical results for helium

Since for two-electron problems accurate *ab initio* calculations are available, the quality of the HCM presented above can be tested by comparing it with results obtained from well-established theoretical methods as well as experiments. As a critical test of the model, we have performed calculations for the double ionization of ground state helium. This test case might be considered, to some extent, the worst case scenario for this model. In the helium ground state, both electrons are equivalent and there is a maximum amount of correlation in the initial state (e.g., it is well known that a simple product wave function ansatz fails by a wide margin to provide the correct shake limit). The picture of a primary electron that absorbs the photon and subsequently scatters off

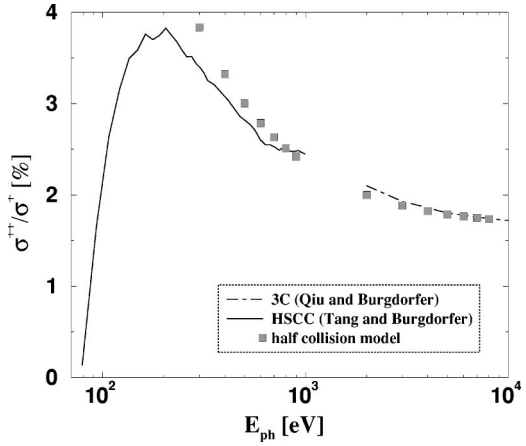

FIG. 1. The ratio σ^{2+}/σ^{+} for helium. Comparison of the HCM results (squares) with accurate *ab initio* data [6].

the second electron appears poorly justified in such a case. One might expect that for more asymmetric electron configurations with less correlation among the electrons, the HCM should perform better. The results of our calculations and the comparison with *ab initio* data are summarized in Figs. 1, 2, and 3.

In Fig. 1, the ratio σ^{2+}/σ^{+} as obtained within the HCM [by a numerical evaluation of Eq. (23)] is compared to a hyperspherical close-coupling calculation at lower energies and a perturbation expansion [6] at high energies. The agreement with these more involved calculations is remarkably good, not only for high energies where, by construction, the HCM will converge to the correct shake limit, but over a surprisingly wide energy range that extends almost down to the maximum of the ratio. Figure 1 can be considered the quantitative realization of the picture originally suggested by Samson [13]. Note, however, that the convergence to the shake limit was absent in the original model.

One can carry this simple picture of sequential ionization a few steps further. In a first step, rather than evaluating

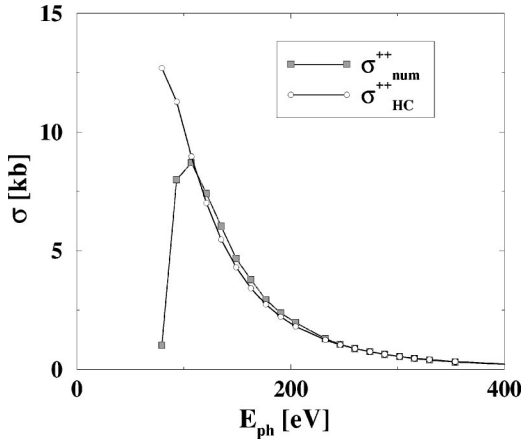

FIG. 2. The helium double-ionization cross section. Comparison of the half-collision model using the electron impact data [Eq. (24)] (circles) with data from a hyperspherical close-coupling calculation (squares). The weight of the electron-impact ionization cross section relative to the shake has been used as a fit parameter, see text for details.

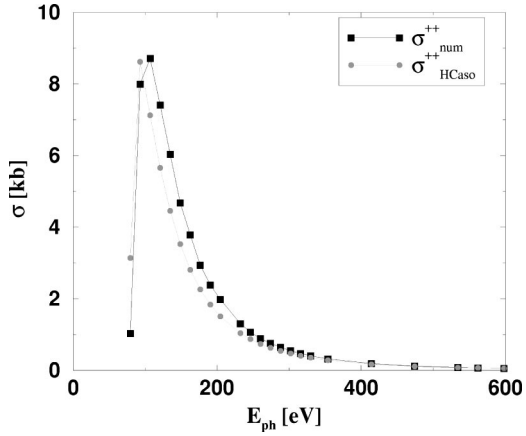

FIG. 3. The helium double-ionization cross section revisited. The hyperspherical close-coupling results (squares) already shown in Fig. 2 are compared to a half-collision calculation with adiabatic switchoff of the shake contribution [Eq. (25)], see text for details.

amplitudes [Eq. (23)] one can further simplify the model by invoking experimental electron-impact ionization cross sections. From $\sigma^{2+}/\sigma^{tot}=R_\infty+k\tilde{\sigma}^{+}$, the ratio can be expressed as

$$\sigma^{2+}/\sigma^{+}=\frac{R_\infty+k\tilde{\sigma}^{+}}{1-R_\infty-k\tilde{\sigma}^{+}}. \tag{24}$$

Here, $\sigma^{tot}=\sigma^{+}+\sigma^{2+}$ is the total photoabsorption cross section, R_∞ is the asymptotic shake limit, and $\tilde{\sigma}^{+}$ the experimental electron-impact ionization cross section of He^{+}. k is an energy-independent proportionality factor relating the cross section for the half-collision to the cross section for the full collision. In Fig. 2, this idea is applied to yield a double-ionization cross section σ^{2+} using σ^{+} from a hyperspherical close-coupling calculation and $\tilde{\sigma}^{+}$ from an electron-impact ionization experiment (where $k=0.00278$ which includes all relevant prefactors relating the transition-matrix element to the cross section). As can be seen, the agreement is remarkably good and extends from the asymptotic limit to the cross section maximum. This simplified picture provides a qualitative underpinning of the HCM.

A second step can be taken to extrapolate such a simplified model to even lower energies, specifically to the region near the cross-section maximum. As one would include the electron-electron interaction to all orders into the T-matrix element of a_{fi}^{II} [Eq. (19)], the separate shake amplitude a_{fi}^{I} [Eq. (16)] should cease to contribute. The shake amplitude contains effects of the electron-electron interaction to all orders, however only in their impulsive limit. As the system undergoes a transition from the sudden to the near-adiabatic limit, those effects represented in the sudden limit (as the speed v of the primary electron goes to infinity) by a^{I} should reappear in a^{II} as v tends to $v_{\text{threshold}}$. The half-collision term then contains the electron-electron interaction to all orders. If now a^{II} is represented by the electron-impact ionization amplitude (or its experimental cross section), a^{I} should be adia-

batically switched off. For an adiabatic switching function we use the function $f_{RZ}(v)=\exp(-2b\,\Delta E/v)$ first introduced by Rosen and Zener in the context of ion-atom collisions (e.g., [21], Chap. 4.9). b signifies here an effective ''impact parameter'' used in the following as a free parameter. With f_{RZ} as switching function and the experimental electron-impact ionization cross section as the ''representative'' of the nonperturbative treatment of the half collision, the ratio of double to single ionization [Eq. (24)] becomes

$$\frac{\sigma^{2+}}{\sigma^{+}}=\frac{R_\infty e^{-2b\Delta E/v}+k\tilde{\sigma}^{+}}{1-R_\infty e^{-2b\Delta E/v}-k\tilde{\sigma}^{+}}. \tag{25}$$

As before, $\tilde{\sigma}^{+}$ refers to the electron-impact single ionization cross section of He^{+}. In Fig. 3, the resulting cross section is compared to the result of a hyperspherical close-coupling calculation. In applying Eq. (25), an analytical parametrization of $\tilde{\sigma}^{+}$ as put forth in Ref. [22] has been used, k is fixed by the requirement to yield the correct slope of the cross section for high energies as calculated within the HCM above. The only free parameter is b, which has been set ''by eye'' to 0.1 to give a favorable fit to the correct cross section. With this simple extension of the half-collision model we reproduce the double ionization from threshold to asymptotically high photon energies (within the nonrelativistic dipole approximation). While, in view of the free parameter involved, the quantitative significance should not be overstated, this model contains the proper physical input and leads to at least qualitatively correct results for all energies. In particular, it leads to the correct shape of the cross section with a single maximum at approximately the correct energy.

At this point, a few further comments about the use of Eq. (23) within the HCM are in order. First, the relatively crude approximation of replacing ϵ_a by an average $\langle\epsilon\rangle$ should be addressed. Even if one accepts this approximation as necessary simplification of the numerical calculation, there is no unique choice for $\langle\epsilon\rangle$ which can be justified *a priori*. In practice, we tested several values of $\langle\epsilon\rangle$ between 24 eV and 55 eV (first and second ionization potential) and found the result to be largely insensitive to the actual value used, in particular for high photon energies. For the lowest energy shown in Fig. 1, the values of σ^{2+}/σ^{+} obtained with different choices of $\langle\epsilon\rangle$ differed by about 11%. One should, however, note that this approximation cannot be used to calculate the transition amplitudes into bound states (i.e., excitation rather than ionization of the second electron) since, depending on the value chosen for $\langle\epsilon\rangle$, different bound final states will come into resonance and the approximation will break down. Instead, one has to invoke a completeness relation to determine the single-ionization cross section as the difference between the total cross section and the double-ionization cross section.

Another critical point is the relative phase between the first-order and second-order term in Eq. (23). In an ordinary Born series, terms of different order N carry a relative phase $\exp[i(N-N')\pi/2]$ and add incoherently for $N-N'$ odd. In the present case of a half-collision, this phase relation is modified and interference terms cannot *a priori* be excluded. Their contribution would be determined by the exact value of the lower limit of the time integral in the half-scattering term. As this value is poorly defined within our model, we omit here and in the following interference terms. There is an additional reason why interference terms are not properly defined in Eq. (23) and, hence, should be omitted. After taking the shake limit, the quantum numbers of the final state of the fast electron have been eliminated (apart from the energy; specifically, l,m in a spherical basis or the emission direction $\hat{\mathbf{k}}_f$ in a plane-wave basis). Inclusion of interference terms resulting from Eq. (23) would therefore overestimate coherences as the final l,m content of the shake and the $e-e$ scattering terms are expected to be different while true coherences would occur only for final states within the same angular momentum sector after integration over all angles.

III. THE THREE-ELECTRON CASE: LITHIUM

In the following section, we will treat the three-electron case of lithium triple ionization. We will first discuss the generalization of the HCM to this more complex breakup process. We will compare our results with experimental data and other theoretical work on the triple ionization problem [10,11].

A. Generalization of the half-collision model

In the previous section, we showed that the half-collision model proposed in this paper is able to give cross sections in surprisingly good agreement with experiments over a wide range of energies, given the simplicity of the model. It seems, therefore, worthwhile to use the model for a calculation of triple ionization cross sections. As discussed above, the ansatz divides the double-ionization process into two sequential processes, namely, (primary) photoionization and a subsequent (secondary) half-collision, which are calculated separately. In the generalization to the three-electron case, which is presented below, an analogous breakdown is attempted. Here we decompose the process in sequences of two-electron processes: as a primary process we consider the double photoionization of the two inner electrons ($1s^2$) of Li (more precisely, of Li^{+} as we ignore the presence of the outer-shell spectator electron in this first step) followed by pair-wise electron-electron scattering at the ''spectator'' $2s$ electron. The second step corresponds to two subsequent *independent* half-collisions of the two primary electrons with the third. This decomposition is both appealing for physical reasons as well as technically convenient. Electron-electron correlations between the two inner electrons are strong while they are very weak with the outer electron. A perturbative treatment of the final-state electron correlation within the framework of the HCM seems therefore appropriate. Furthermore, the inner and outer electrons in Li are well separated in both coordinate space ($\langle r\rangle_{1s}/\langle r\rangle_{2s}\ll 1$) as well as energy space (the binding energy $E_B(1s^2)$ accounts for 97% of the

total binding energy). From a technical point of view, this decomposition allows the usage of *ab initio* methods of two-electron systems for double ionization in the first step, thereby accounting for electron correlations in both the initial state and final state as well as the energy sharing between these electrons accurately while neglecting the spectator electron. The triple ionization cross section is calculated as

$$\sigma^{3+}(\mathrm{Li}) = \frac{\sigma^{3+}}{\sigma^{2+}} \sigma^{2+}(\mathrm{Li}^{+}), \tag{26}$$

where $\sigma^{2+}(\mathrm{Li}^{+})$ is taken from *ab initio* methods while the ratio σ^{3+}/σ^{2+} is determined by the HCM.

An important point to be noted with reference to Eq. (26) is that $\sigma^{2+}(\mathrm{Li}^{+})$ refers to true double ionization in a two-electron system as opposed to two-electron removal in the neutral three-electron system, i.e., $\sigma^{2+}(\mathrm{Li})$. Unlike $\sigma^{2+}(\mathrm{Li}^{+})$, the double ionization of neutral Li includes a significant contribution from indirect processes of inner-shell single ionization followed by Auger decay.

The treatment of triple ionization within the HCM proceeds in close analogy to the two-electron case. In analogy to Eqs. (1) to (7), we denote the initial and final states by

$$|\Psi_i\rangle = |\psi_i(1,2,3) n_{\omega,\sigma} = 1\rangle, \tag{27}$$

$$|\Psi_f\rangle = |\phi_f(1)\psi_f(2,3) n_{\omega,\sigma} = 0\rangle. \tag{28}$$

The model Hamiltonian for the HCM for Li–like systems reads

$$H = h(1) + h(2) + h(3) + h_{ph} + V_{ee}^{(1,2)} + V_{ee}^{(1,3)} + V_{ee}^{(2,3)} + W^{(2,3,ph)}. \tag{29}$$

The channel Hamiltonians for the entrance (α) and exit (β) channel are

$$H^{\alpha} = h(1) + h(2) + h(3) + h_{ph} + V_{ee}^{(1,2)} + V_{ee}^{(1,3)} + V_{ee}^{(2,3)} \tag{30}$$

and

$$H^{\beta} = h(1) + h(2) + h(3) + h_{ph} + V_{ee}^{(2,3)}. \tag{31}$$

The corresponding channel perturbations read

$$V^{\alpha} = H - H^{\alpha} = W^{(2,3,ph)} \equiv \frac{1}{c}(\mathbf{p}_2 + \mathbf{p}_3)\cdot\mathbf{A} \tag{32}$$

and

$$V^{\beta} = H - H^{\beta} = V_{ee}^{(1,2)} + V_{ee}^{(1,3)} + \frac{1}{c}(\mathbf{p}_2 + \mathbf{p}_3)\cdot\mathbf{A}. \tag{33}$$

Labeling the outer electron by 1 and the inner electrons by 2 and 3, the amplitude for triple ionization within the HCM to first order in the electron-electron interaction V_{ee} is given by

$$a_{fi} = -i\int_{-\infty}^{\infty} dt\, e^{i(E_f^{tot} - E_i^{tot})t} \langle \psi_f | \frac{1}{c}(\mathbf{p}_2 + \mathbf{p}_3)\cdot\mathbf{A} | \psi_i \rangle - \int_{-\infty}^{\infty} dt_1 \int_{t_1}^{\infty} dt_2 e^{i(E_f^{tot} t_2 - E_i^{tot} t_1)} \langle \psi_f | (V_{ee}^{(1,2)} + V_{ee}^{(1,3)}) e^{-iH^{\beta} t_2} e^{iH^{\beta} t_1} \frac{1}{c}(\mathbf{p}_2 + \mathbf{p}_3)\cdot\mathbf{A} | \psi_i \rangle. \tag{34}$$

As in the double-ionization case treated in Sec. II, in the following discussion we consider the outer (secondary) electron (1) to be distinguishable from the two inner (primary) electrons (2,3) and neglect antisymmetrization. The first term represents the shake amplitude, while the second term contains the additional electron-electron scattering between the ejected electrons and the spectator electron. In Eq. (28) we have used the assumption that the spectator electron is weakly correlated with the pair of inner-shell electrons in the final state such that the wave function can be factorized. If we now employ a similar approximation for the initial state

$$|\psi_i(1,2,3)\rangle = |\phi_i(1)\psi_i(2,3)\rangle, \tag{35}$$

the first term in the transition amplitude factorizes into the amplitude for double ionization of the inner electrons times an asymptotic one-electron shake factor for the spectator electron,

$$a_{fi}^{I} = -2\pi i\, \delta(E_f - E_i - \omega_{ph}) \langle \psi_f(2,3) | \frac{1}{c}(\mathbf{p}_2 + \mathbf{p}_3)\cdot\mathbf{A} | \psi_i(2,3) \rangle \times \langle \phi_f(1) | \phi_i(1) \rangle. \tag{36}$$

It is important to note that in the present treatment the ionization dynamics of the $(1s^2)$ is taken into account accurately (save for the presence of the spectator electron). The shake approximation is only invoked for the spectator electron. The shake factor is given by the overlap between the $2s$ single-particle orbital of the neutral lithium $|\phi_i(1)\rangle$ with the hydrogenic (bound or continuum) orbitals $|\phi_f(1)\rangle$ of the doubly ionized Li.

The second term in Eq. (34) can be written as a product of the amplitude for photoionization to an intermediate continuum state $(\mathbf{k}_n, \mathbf{k}_o)$ followed by the electron-impact ionization of the spectator electron $[\phi_{\mathbf{k}_n}(\mathbf{r}_2) \equiv (1/(2\pi)^{3/2}) e^{i\mathbf{k}_n\cdot\mathbf{r}_2}]$

$$a_{fi}^{II} \propto \sum_{j=2}^{3} \sum\!\!\!\!\!\!\int_{\mathbf{k}_n,\mathbf{k}_0} \langle \psi_f | V_{ee}^{(1,j)} | \phi_i(1)\phi_{\mathbf{k}_n}(2)\phi_{\mathbf{k}_o}(3) \rangle \times \langle \phi_{\mathbf{k}_n}(2)\phi_{\mathbf{k}_o}(3) | \frac{1}{c}(\mathbf{p}_2 + \mathbf{p}_3)\cdot\mathbf{A} | \psi_i(2,3) \rangle. \tag{37}$$

The notation in Eq. (37) is rather sloppy in that we did not write the integrations and phase factors related to t_1 and t_2 that appear in Eq. (34) for the sake of a simpler notation. They are treated exactly as in the two-electron case [Eqs. (17), (20), and (22)]. In Eqs. (36) and (37), we use as single-particle orbital for the initial state of the spectator electron, a Roothaan Hartree Fock wave function

$$\phi_i(\mathbf{r}_1)=\left(\sum_{j=1}^{2} c_j e^{-\alpha_j r}+\sum_{j=3}^{6} c_j r e^{-\alpha_j r}\right) Y_{00} \tag{38}$$

with the coefficients c_j and α_j for the $2s$ orbital given in Ref. [23] with binding energy $\epsilon_i=-0.1981$ a.u. The final state ϕ_f is a hydrogenic bound or continuum orbital in the field of the bare Li nucleus.

The half-scattering amplitude in Eq. (37) is evaluated in the same way as in the two-electron case, namely, in first-order time-dependent perturbation theory treating V_{ee} as a time-dependent perturbation

$$V_{ee}^{(1,i)}(t)=\frac{1}{|\mathbf{r}_1-\mathbf{k}_i t|}, \tag{39}$$

where the outward trajectory of the "projectile" electron starts near the nucleus with zero impact parameter relative to the nucleus. Details of the evaluation of the matrix elements for the half-scattering amplitude can be found in the appendices.

We employ a Fourier transform of the final-state wave function $\psi_f(\mathbf{r}_2,\mathbf{r}_3)$

$$\begin{aligned}\psi_f(\mathbf{r}_2,\mathbf{r}_3)&=\frac{1}{(2\pi)^6}\int d^3k_3\int d^3k_2,\tilde{\psi}_f(\mathbf{k}_2,\mathbf{k}_3)\mathrm{e}^{i\mathbf{k}_2\cdot\mathbf{r}_2}\mathrm{e}^{i\mathbf{k}_3\cdot\mathbf{r}_3}\\&\equiv\frac{1}{(2\pi)^3}\int d^3k_3\int d^3k_2\tilde{\psi}_f(\mathbf{k}_2,\mathbf{k}_3)\phi_{\mathbf{k}2}(\mathbf{r}_2)\phi_{\mathbf{k}3}(\mathbf{r}_3).\end{aligned} \tag{40}$$

We make the further approximation that the outer secondary electron will be slow and electrons 2 and 3 share the total energy [see also the discussion following Eq. (22)],

$$k_2^2+k_3^2=2E, \tag{41}$$

so that

$$\begin{aligned}\psi_f(\mathbf{r}_2,\mathbf{r}_3)=\frac{1}{(2\pi)^6}\int d\Omega_3\int d^3k_2\tilde{\psi}_f(\mathbf{k}_2,\mathbf{k}_3)\\\times e^{i\mathbf{k}_2\cdot\mathbf{r}_2}e^{i\sqrt{2E-k_2^2}\hat{\mathbf{k}}_3\cdot\mathbf{r}_3}.\end{aligned} \tag{42}$$

Inserting Eq. (42) into the first matrix element of Eq. (37), we are then left with expressions of the form

$$\begin{aligned}&\langle\phi_f(1)\phi_{\mathbf{k}_2}(2)\phi_{\mathbf{k}_3}(3)|V_{ee}^{(1,2)}|\phi_i(1)\phi_{\mathbf{k}_n}(2)\phi_{\mathbf{k}_o}(3)\rangle\\&=\langle\phi_f(1)\phi_{\mathbf{k}_2}(2)|V_{ee}^{(1,2)}|\phi_m(1)\phi_{\mathbf{k}_n}(2)\rangle\delta(\mathbf{k}_3-\mathbf{k}_o)\end{aligned} \tag{43}$$

and a similar expression involving $V_{ee}^{(1,3)}$. Subsequent integration over d^3k_o eliminates the δ distribution. The remaining bracket on the right-hand side of Eq. (43) is thus reduced to a two-particle matrix element similar to that for the two-electron problem. The only difference to Eq. (18) is that the expansion (40) requires an additional integration over $d^3k_2d\Omega_3$. The half-collision part of Eq. (37) is thus written as a sum of two independent half-collisions of the outer electron with electron 2 and electron 3, respectively,

$$\begin{aligned}a_{fi}^{II}\propto\sum_{\mathbf{k_n},\mathbf{k_0}}\int d\Omega_3\int d^3k_2\tilde{\psi}_f(\mathbf{k_2},\mathbf{k_3})\Bigg(\underbrace{\langle\phi_f(1)\phi_{\mathbf{k_2}}(2)|V_{ee}^{(1,2)}|\phi_i(1)\phi_{\mathbf{k_n}}(2)\rangle}_{\text{half coll. with } v=k_2}+(\mathbf{k_2}\leftrightarrow\mathbf{k_3})\Bigg)\\\times\langle\phi_{\mathbf{k_n}}(2)\phi_{\mathbf{k_o}}(3)|\tfrac{1}{c}(\mathbf{p_2}+\mathbf{p_3})\cdot\mathbf{A}|\psi_i(2,3)\rangle.\end{aligned} \tag{44}$$

Within the impact-parameter approximation employed here, the resulting half-collision transition probabilities into a final state with given energy for the secondary electron (i.e., after summation over l,m) do not depend on the directions $\hat{\mathbf{k}}_2$ and $\hat{\mathbf{k}}_3$. Physically, this can be seen from the fact that the initial state is spherically symmetric, so after the complete process has been broken down into independent two-electron collisions, the only physically preferred axis is the direction of

the outgoing ''projectile.'' Mathematically, it relies on the fact that $\Sigma_m Y_{lm}^*(\Omega)Y_{lm}(\Omega)=(2l+1)/(4\pi)$ is invariant under rotation. The half-collision integral then selects final states that have $m=0$ with respect to the direction of the ''projectile'' as the quantization axis (see Appendix C). It is, however, important to note that this independence of the half-collision transition probabilities of the directions $\hat{\mathbf{k}}_2$ and $\hat{\mathbf{k}}_3$ (after summation over m as discussed above) holds only for the secondary electron, which has to be clearly distinguished from the photoabsorption process, which does, of course, not lead to isotropic emission of the primary electrons. The argument therefore relies on the factorization of the final state, which allows for an independent summation over final states for the primary and secondary electrons, respectively. In this case, we can define the energy sharing distribution of the primary electrons:

$$P(\epsilon)\equiv\sum_f\left|\int d\Omega_3\int d\Omega_2\int d^3r_3 \times\int d^3r_2\,\psi_f(\mathbf{r}_2,\mathbf{r}_3)e^{i\mathbf{k}_2\cdot\mathbf{r}_2}e^{i\sqrt{2E-k_2^2}\hat{\mathbf{k}}_3\cdot\mathbf{r}_3}\right|^2, \quad (45)$$

where $\epsilon=k_2^2/2$ is the energy of the slower of the two primary electrons and the summation is over the final states of the *primary* electrons only. The half-collision contribution to the transition probability can then be obtained by integrating over the energy sharing $P(\epsilon)$.

With the amplitudes evaluated according to Eqs. (36) and (44), the cross section ratio σ^{3+}/σ^{2+} is then given by summing over continuum ($\phi_{k,l}$) and bound ($\phi_{n,l}$) final states, respectively. Using the same approximations, namely, a closure approximation for the intermediate states and incoherent addition of shake and half-collision contributions, discussed in detail for the two-electron case, we finally have

$$\frac{\sigma^{3+}}{\sigma^{2+}}=\frac{\sum_l\int dk\,k|\langle\phi_{k,l}|\phi_i\rangle|^2+\sum_l\int dk\,k\int d\epsilon\,P(\epsilon)\left|\int_0^\infty dt\left\langle\phi_{k,l}\left|e^{i(k^2/2-E_i)t}\left(\frac{1}{|\mathbf{r}-\sqrt{2\epsilon}t\mathbf{e}_z|}+\frac{1}{|\mathbf{r}-\sqrt{2(E-\epsilon)}t\mathbf{e}_z|}\right)\right|\phi_i\right\rangle\right|^2}{\sum_{l,n}|\langle\phi_{n,l}|\phi_i\rangle|^2+\sum_{l,n}\int d\epsilon\,P(\epsilon)\left|\int_0^\infty dt\left\langle\phi_{n,l}\left|e^{i(-Z^2/(2n^2)-E_i)t}\left(\frac{1}{|\mathbf{r}-\sqrt{2\epsilon}t\mathbf{e}_z|}+\frac{1}{|\mathbf{r}-\sqrt{2(E-\epsilon)}t\mathbf{e}_z|}\right)\right|\phi_i\right\rangle\right|^2}. \quad (46)$$

The incoherent addition of shake and half-collision contributions has already been discussed in the two-electron case. The same argument, namely, avoidance of double counting, applies to the integration of the half-collision probabilities (rather than amplitudes) over the energy sharing distribution $P(\epsilon)$, which already involves a summation over different final states for the primary electrons. The double-ionization cross section for Li^+ does not explicitly appear in the ratio Eq. (46). However, it enters implicitly through the energy sharing distribution $P(\epsilon)$ of the ejected primary electrons from Li^+ in its ground state. Since σ^{2+} for Li^+ can be independently and accurately calculated, the absolute triple ionization cross section can be determined using Eqs. (46) and (26).

B. Results and discussion

The validity of first-order perturbation theory in the $e-e$ interaction for triple ionization underlying Eq. (46) is *a priori* not obvious. Even in the limit $E_{ph}\to\infty$, the energy sharing in double ionization is strongly asymmetric (''*U* shaped''), consisting of a slow and a fast electron, which give rise to different half-collision contributions with the slow electron providing the dominant term. For the extreme low-energy tail, the perturbation theory breaks down. We have therefore introduced, in the energy integral in Eq. (46), a low cutoff $\epsilon>\epsilon_c$, thereby excluding the most asymmetric energy sharing contributions. This cutoff is not only required to suppress spurious contributions from the breakdown of perturbation theory but also to exclude contributions that are inconsistent with the threshold for impact ionization. Within the HCM, the ''projectile'' (i.e., the departing electron) must have an energy in excess of the threshold for ionization of the spectator electron. ϵ_c should be somewhat larger than the initial binding energy of the 2*s* electron in neutral Li because the screening of the nuclear charge due to the two 1*s* electrons is no longer operative during the half-collision. Moreover, the assumption of a projectile moving with a (near)

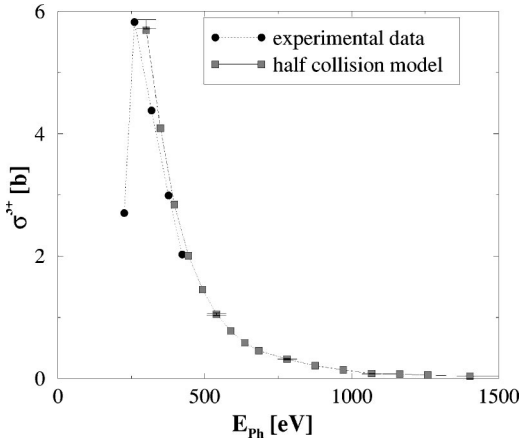

FIG. 4. The triple ionization cross section of lithium: experimental data (circles) and HCM results (squares). At 301, 540, 780, and 1068 eV photon energy, error bars indicate the effect of different cutoff energies ϵ_c.

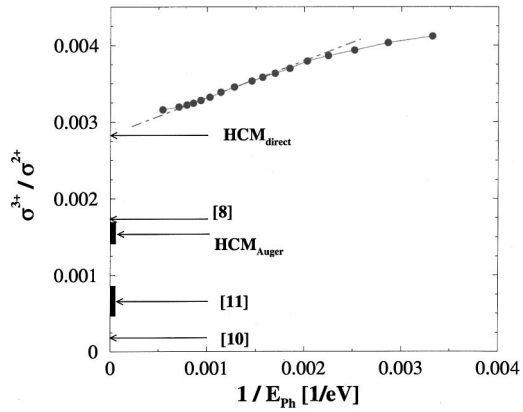

FIG. 5. The ratio σ^{3+}/σ^{2+} for photoionization of lithium as a function of $1/E$. The high-energy limits given in Refs. [8,10,11] are indicated. Note that the HCM does not include contributions to σ^{2+} from indirect processes, see text for a discussion. Tentatively taking them into account on the basis of Ref. [10] leads to a reduced ratio, the high-energy limit of which is denoted by HCM_{Auger} (the ''error bar'' here corresponds to the range 40% to 50% indirect contributions stated in Ref. [10]).

constant well-defined velocity underlying the impact-parameter approximation becomes questionable for slow primary electrons due to their intrinsic momentum spread (Compton profile). Near the radius of the 2*s* electron where the collision will take place, the projectile will have a higher kinetic energy balancing the potential energy at intermediate distances from the nucleus. A precise value for a lower bound ϵ_c cannot be given, however, as we show below, we found that the final result is remarkably insensitive to the value used.

Figure 4 displays the resulting triple ionization cross section in comparison with recent experimental data [8]. The theoretical error bar represents variation for different choices of ϵ_c varying between 0.4 and 1 a.u. The uncertainty in the final result for σ^{3+} does not exceed $\approx 10\%$, which is well within the overall uncertainty we can expect from the simple HCM. The agreement for energies above the cross section maximum ($E_{ph} > 300$ eV) is again remarkably good considering the simplicity of the model.

The ratio σ^{3+}/σ^{2+} is a smoothly decreasing function (Fig. 5). This smooth energy dependence suggests the extrapolation to $E_{ph} \to \infty$, which allows a comparison with previous estimates for the asymptotic ''shake-off'' limit [10,11] in close analogy to the case of double ionization in two-electron systems [24–26]. In Fig. 5 we present a smooth $1/E_{ph}$ extrapolation of this ratio to zero which should, however, be taken with caution since a numerically stable evaluation of Eq. (46) is difficult to achieve as $E_{ph} \to \infty$ and therefore could not be directly verified. The indicated limit differs from the previous estimates. Cooper [11] has calculated asymptotic shake probabilities by assuming that both inner-shell electrons are removed instantaneously, i.e., a double-shake process. He used for the spectator electron Hartree Fock wave functions to describe the initial state and projected them onto hydrogenic final states. This approach closely resembles the first term a_{fi}^{I} [Eq. (36)]. However, the HCM does not converge to this limit since the final-state Coulomb correlation represented by a_{fi}^{II} does not vanish as $E_{ph} \to \infty$. Van der Hart and Greene [10] have calculated the triple-ionization probability by representing the lithium ground state and the final states of the residual two-electron Li^+ system (bound states, single continuum, double continuum) by *B* splines. For the fast electron instant removal, i.e., the shake limit, is assumed. Transition amplitudes have then been calculated in terms of overlap integrals between the ground state (with $\mathbf{r}_3 = 0$) and the various final states in Li^+. This method features a more accurate representation of the initial state as well as the final state of the ''slow'' electron in the double ejection process. On the other hand, this method neglects any residual interaction of a ''fast'' electron with any of the residual electrons, i.e., half-scattering with the spectator electron as well as the electron-electron correlation in the final state of the $(1s^2)$ two-electron pair. When comparing results for σ^{3+}/σ^{2+}, it is important to realize that Ref. [10] includes indirect processes contributing to $\sigma^{2+}(\mathrm{Li})$, namely via the excitation of doubly excited states and subsequent autoionization. It was estimated in Ref. [10] that they account for more than 40% of all double-ionization events, so that the ratio of triple to double ionization would be roughly a factor of 2 smaller than the one shown as HCM_{direct} in Fig. 5, which uses $\sigma^{2+}(Li^+)$. Applying this correction to the HCM (denoted by HCM_{Auger} in Fig. 5) brings our data in the range of the experimentally observed ratios at finite energies. However, our high-energy data would still differ from the previous estimates, even though by a smaller amount. A direct comparison of the asymptotic ratios is further complicated by the fact that the method of Ref. [10] as well as ours require additional technical approximations in the evaluation (an approximate ''incoherent'' projection of Li^+ orbitals onto hydrogenic orbitals and the indirect determination of triple ionization by subtraction in Ref. [10], and the closure approximation for intermediate states in the present HCM). Clearly, more comprehensive numerical studies are required to determine the high-energy limit more accurately.

IV. CONCLUSIONS AND OUTLOOK

In this paper, we have presented the half-collision model for the calculation of multiple ionization by single-photon absorption. The model is based on a simple and appealing underlying physical picture. It can be derived from a high-energy approximation in the framework of a Born-type perturbation series. In a benchmark calculation for helium double ionization, we have shown that the HCM is capable of producing cross sections in remarkable agreement with experiments and other more elaborate numerical calculations over a surprisingly wide energy range. We furthermore applied the model to the triple ionization of lithium, where again the results compared favorably with recent experiments. Previous calculations have been limited to the high-energy limit, which was assumed to be approached only for several keV photon energy. In this high-energy limit, our results differ from those previously obtained, which can only in part be attributed to the neglect of indirect processes lead-

ing to doubly excited intermediate states that eventually autoionize and contribute to the double-ionization cross section.

One future direction for application of the HCM is multiple ionization in intense laser fields. Rescattering at core electrons of the field-ionized primary electron has been shown to be the dominant multiple ionization mechanism. Such a process could be treated within an analog to the HCM presented here.

ACKNOWLEDGMENTS

It is a pleasure to thank R. Wehlitz, Y. Azuma, M.-T. Huang, and I.A. Sellin for helpful discussions. Financial support by the Grant No. NSF PHY 9805197 and the FWF SFB 016 is gratefully acknowledged.

APPENDIX A: MULTICHANNEL SCATTERING THEORY

For the sake of completeness of the derivation, we give a summary of the essential steps leading to the series expression (13) for the transition amplitude. The content of this appendix employs standard multichannel scattering theory (e.g., Ref. [15]) taylored to our specific problem.

We start from the general expression (12). Let us define the operator

$$s(t) \equiv e^{iH^\beta T} U(T,t) e^{-iH^\alpha t} \tag{A1}$$

from which we will finally get

$$S = \lim_{T\to\infty T'\to-\infty} s(T'). \tag{A2}$$

Using the relation $i\partial_t U(T,t) = -HU(T,t)$ for the time evolution operator, we obtain

$$\begin{aligned}\partial_t s(t) &= e^{iH^\beta T} U(T,t) iH\, e^{-iH^\alpha t} + e^{iH^\beta T} U(T,t)(-iH^\alpha) e^{-iH^\alpha t} \\ &= e^{iH^\beta T} U(T,t) i(H-H^\alpha) e^{-iH^\alpha t} \\ &= i\, e^{iH^\beta T} U(T,t) V^\alpha e^{-iH^\alpha t}.\end{aligned} \tag{A3}$$

This leads to

$$\begin{aligned}s(T') &= s(T) - \int_{T'}^{T} dt_1 \partial_t s(t_1) \\ &= e^{iH^\beta T} e^{-iH^\alpha T} - i\int_{T'}^{T} dt_1 e^{iH^\beta T} U(T,t_1) V^\alpha e^{-iH^\alpha t_1} \\ &= e^{iH^\beta T} e^{-iH^\alpha T} - i\int_{T'}^{T} dt_1 e^{iH^\beta T} U(T,t_1) e^{-iH^\beta t_1} \\ &\quad \times e^{iH^\beta t_1} V^\alpha e^{-iH^\alpha t_1}.\end{aligned} \tag{A4}$$

Similarly, we use

$$\begin{aligned}\partial_t [e^{iH^\beta T} U(T,t) e^{-iH^\beta t}] &= e^{iH^\beta T} U(T,t)(iH) e^{-iH^\beta t} \\ &\quad - e^{iH^\beta T} U(T,t)(iH^\beta) e^{-iH^\beta t} \\ &= i\, e^{iH^\beta T} U(T,t) V^\beta e^{-iH^\beta t}\end{aligned} \tag{A5}$$

to get

$$\begin{aligned}\tilde{U}(t_1) &\equiv e^{iH^\beta T} U(T,t_1) e^{-iH^\beta t_1} \\ &= e^{iH^\beta T} e^{-iH^\beta T} - i\int_{t_1}^{T} dt_2 e^{iH^\beta T} U(T,t_2) V^\beta e^{-iH^\beta t_2} \\ &= 1 - i\int_{t_1}^{T} dt_2 e^{iH^\beta T} U(T,t_2) e^{-iH^\beta t_2} e^{iH^\beta t_2} V^\beta e^{-iH^\beta t_2} \\ &= 1 - i\int_{t_1}^{T} dt_2 \tilde{U}(t_2) e^{iH^\beta t_2} V^\beta e^{-iH^\beta t_2}.\end{aligned} \tag{A6}$$

Repeatedly using this relation in Eq. (A4), we obtain a Born series expression for $s(T)$. Note that this series contains only first-order terms in V^α (the ''weak potential''), but arbitrary orders in the electron-electron interaction. To second order, Eq. (A4) reads

$$\begin{aligned}s(T') &= e^{iH^\beta T} e^{-iH^\alpha T} - i\int_{T'}^{T} dt_1 e^{iH^\beta t_1} V^\alpha e^{-iH^\alpha t_1} \\ &\quad + (-i)^2 \int_{T'}^{T} dt_1 \int_{t_1}^{T} dt_2 e^{iH^\beta t_2} V^\beta e^{-iH^\beta t_2} e^{iH^\beta t_1} V^\alpha \\ &\quad \times e^{-iH^\alpha t_1} + \cdots.\end{aligned} \tag{A7}$$

Thus, with Eq. (11) and Eq. (A2) the transition amplitude can be expressed as

$$\begin{aligned}a_{fi} &= \lim_{T\to\infty\ T'\to-\infty} \langle \phi_f(1)\phi_{\mathbf{k}_f}(2) n_{\omega,\sigma} = 0 \\ &\quad \times |e^{iH^\beta T} e^{-iH^\alpha T}| \psi_i(1,2) n_{\omega,\sigma} = 1\rangle \\ &\quad + \left\langle \phi_f(1)\phi_{\mathbf{k}_f}(2) n_{\omega,\sigma} = 0 \right| \\ &\quad - i\int_{T'}^{T} dt_1 e^{iH^\beta t_1} V^\alpha e^{-iH^\alpha t_1} \left| \psi_i(1,2) n_{\omega,\sigma} = 1 \right\rangle \\ &\quad + \left\langle \phi_f(1)\phi_{\mathbf{k}_f}(2) n_{\omega,\sigma} = 0 \right| (-i)^2 \\ &\quad \times \int_{T'}^{T} dt_1 \int_{t_1}^{T} dt_2 e^{iH^\beta t_2} V^\beta e^{-iH^\beta t_2} e^{iH^\beta t_1} V^\alpha \\ &\quad \times e^{-iH^\alpha t_1} \left| \psi_i(1,2) n_{\omega,\sigma} = 1 \right\rangle + \cdots\end{aligned} \tag{A8}$$

which is Eq. (13).

APPENDIX B: AN IMPACT-PARAMETER APPROXIMATION FOR THE HALF-COLLISION INTEGRAL

As discussed in Sec. II, for high photon energies the primary electron is very fast when leaving the target and its trajectory will be perturbed only slightly by the Coulomb interaction with the secondary electron. Since the naive picture is that of the primary electron first absorbing the photon, thereby being in a high-energy continuum state, it seems reasonable to make the assumption that the matrix element $\langle \psi_{ab} n_{\omega,\sigma}=0 | (1/c)\mathbf{p}_2\cdot\mathbf{A} | \psi_i n_{\omega,\sigma}=1\rangle$ peaks at energies $E_{ab}\approx E_f$ that are high enough that the corresponding ψ_{ab} can be approximated by a product wavefunction $(1/\sqrt{(2\pi)^3})\phi_a(\mathbf{r}_1)\phi_{\mathbf{k}}(\mathbf{r}_2)$. Moreover, we also assume that the electron-electron interaction will only be a small perturbation, so that $\mathbf{k}\approx\mathbf{k}_f$. The integral in Eq. (18) can then be written as

$$
\begin{aligned}
I_{fi}^{II} \equiv & \sum\!\!\!\!\!\!\int_{a,b} \int_0^\infty dt\, e^{i(E_f-E_{ab})t} \langle \phi_f(1)\phi_{\mathbf{k}_f}(2)|V_{ee}|\psi_{ab}(1,2)\rangle \\
& \times \left\langle \psi_{ab}(1,2) n_{\omega,\sigma}=0 \left| \frac{1}{c}\mathbf{p}_2\cdot\mathbf{A} \right| \psi_i(1,2) n_{\omega,\sigma}=1 \right\rangle \\
= & \sum\!\!\!\!\!\!\int_a \int d^3k \int_0^\infty dt\, e^{i(k_f^2/2+\epsilon_f-k^2/2-\epsilon_a)t} \\
& \times \langle \phi_f(1)\phi_{\mathbf{k}_f}(2)|V_{ee}^{(1,2)}|\phi_a(1)\phi_{\mathbf{k}}(2)\rangle \\
& \times \left\langle \phi_a(1)\phi_{\mathbf{k}}(2) n_{\omega,\sigma}=0 \left| \frac{1}{c}\mathbf{p}_2\cdot\mathbf{A} \right| \psi_i(1,2) n_{\omega,\sigma}=1 \right\rangle .
\end{aligned}
\tag{B1}
$$

The second matrix element is evaluated in the high-energy limit analogous to the first-order term and yields

$$
\begin{aligned}
& \left\langle \phi_a(1)\phi_{\mathbf{k}}(2) n_{\omega,\sigma}=0 \left| \frac{1}{c}\mathbf{p}_2\cdot\mathbf{A} \right| \psi_i(1,2) n_{\omega,\sigma}=1 \right\rangle \\
& \qquad \rightarrow \left(\frac{2\pi}{L}\right)^{3/2} 4\sqrt{2} Z \cos(\gamma) k^{-4} \\
& \qquad \times \langle \phi_a | \psi_i(1,\mathbf{r}_2=0)\rangle .
\end{aligned}
\tag{B2}
$$

(Here and in the remainder of this appendix, we denote the angles between the photon polarization vector and $\mathbf{k}$ and $\mathbf{k}_f$ as γ and γ_f, respectively.) This leads to

$$
\begin{aligned}
I_{fi}^{II} = & \left(\frac{2\pi}{L}\right)^{3/2} 4\sqrt{2} Z \sum\!\!\!\!\!\!\int_a \langle \phi_a | \psi_i(1,\mathbf{r}_2=0)\rangle \\
& \times \int_0^\infty dt\, e^{i(\epsilon_f-\epsilon_a)t} \int d^3k \cos(\gamma)\, k^{-4} e^{i(k_f^2/2-k^2/2)t} \\
& \times \left\langle \phi_f(1)\phi_{\mathbf{k}_f}(2) \left| \frac{1}{|\mathbf{r}_1-\mathbf{r}_2|} \right| \phi_a(1)\phi_{\mathbf{k}}(2) \right\rangle ,
\end{aligned}
\tag{B3}
$$

where we have inserted the Coulomb interaction V_{ee}. In order to evaluate the matrix element

$$
\begin{aligned}
& \left\langle \phi_f(1)\phi_{\mathbf{k}_f}(2) \left| \frac{1}{|\mathbf{r}_1-\mathbf{r}_2|} \right| \phi_a(1)\phi_{\mathbf{k}}(2) \right\rangle \\
& \qquad = \frac{1}{(2\pi)^3} \int d^3r_2 \int d^3r_1 \frac{\phi_f^*(\mathbf{r}_1)\phi_a(\mathbf{r}_1)}{|\mathbf{r}_1-\mathbf{r}_2|} e^{i(\mathbf{k}-\mathbf{k}_f)\cdot\mathbf{r}_2},
\end{aligned}
\tag{B4}
$$

let us choose $\mathbf{k}_f$ along the z direction and assume $\mathbf{k}\approx\mathbf{k}_f$. Then $\mathbf{k}_f\cdot\mathbf{r}_2 = k_f z_2$ and $\mathbf{k}\cdot\mathbf{r}_2 \approx k z_2$, so that (see Ref. [21] for an analogous treatment)

$$
(\mathbf{k}-\mathbf{k}_f)\cdot\mathbf{r}_2 \approx k_x x_2 + k_y y_2 + (k-k_f) z_2 \tag{B5}
$$

$[k_x \equiv (\mathbf{k})_x, k_y \equiv (\mathbf{k})_y, k_z \equiv (\mathbf{k})_z]$. Moreover, we have

$$
k^2 - k_f^2 = k^2 - [k+(k_f-k)]^2 \approx 2k(k-k_f), \tag{B6}
$$

i.e.,

$$
k - k_f \approx \frac{k^2-k_f^2}{2k} \equiv \frac{k^2-k_f^2}{2v}. \tag{B7}
$$

After substituting $z_2 = v\tau$ in Eq. (B4), insertion of Eq. (B4) into Eq. (B3) and the use of $\mathbf{k}\approx\mathbf{k}_f$ to replace $\cos(\gamma)k^{-4}$ by $\cos(\gamma_f)k_f^{-4}$, leads to

$$
\begin{aligned}
I_{fi}^{II} = & \frac{1}{(2\pi)^3} \left(\frac{2\pi}{L}\right)^{3/2} 4\sqrt{2} Z \sum\!\!\!\!\!\!\int_a \langle \phi_a | \psi_i(1,\mathbf{r}_2=0)\rangle \\
& \times \int_0^\infty dt\, e^{i(\epsilon_f-\epsilon_a)t} \int d^3r_1 \int dy_2 \int dx_2 \int d\tau \int d^3k \\
& \times \frac{\phi_f^*(\mathbf{r}_1)\phi_a(\mathbf{r}_1)}{[(x_1-x_2)^2+(y_1-y_2)^2+(z_1-v\tau)^2]^{(1/2)}} \\
& \times \cos(\gamma_f) k_f^{-4} e^{i(k_x x_2 + k_y y_2)} e^{i(k_f^2/2-k^2/2)(t-\tau)v}.
\end{aligned}
\tag{B8}
$$

Since

$$
v\, dk_z = k\, dk_z \approx k\, dk = d(k^2/2) \tag{B9}
$$

we have

$$
\int dk_z e^{i(k_f^2/2-k^2/2)(t-\tau)v} \approx 2\pi\delta(t-\tau). \tag{B10}
$$

Subsequent integration over τ then leads to

$$I_{fi}^{II}=\frac{1}{(2\pi)^3}\left(\frac{2\pi}{L}\right)^{3/2}4\sqrt{2}Z\cos(\gamma_f)k_f^{-4}\sum\!\!\!\!\!\!\int_a\langle\phi_a|\psi_i(1,\mathbf{r}_2=0)\rangle\int_0^\infty dt\,e^{i(\epsilon_f-\epsilon_a)t}\int d^3r_1\int dy_2\int dx_2$$

$$\times\frac{\phi_f^*(\mathbf{r}_1)\phi_a(\mathbf{r}_1)}{[(x_1-x_2)^2+(y_1-y_2)^2+(z_1-vt)^2]^{(1/2)}}\int dk_y\int dk_x e^{i(k_xx_2+k_yy_2)}2\pi$$

$$=\frac{1}{(2\pi)^2}\left(\frac{2\pi}{L}\right)^{3/2}4\sqrt{2}Z\cos(\gamma_f)k_f^{-4}\sum\!\!\!\!\!\!\int_a\int_0^\infty dt\int dy_2\int dx_2 e^{i(\epsilon_f-\epsilon_a)t}\langle\phi_a|\psi_i(1,\mathbf{r}_2=0)\rangle$$

$$\times\langle\phi_f(1)|V_{ee}(1,\mathbf{r}_2=(x_2,y_2,vt))|\phi_a(1)\rangle\int dk_y\int dk_x e^{i(k_xx_2+k_yy_2)}. \tag{B11}$$

In order to perform the integrals over the transverse coordinates x_2 and y_2, let us now write

$$k_x\equiv v\sin(\Theta)\cos(\alpha),\quad k_y\equiv v\sin(\Theta)\sin(\alpha),$$
$$k_z\equiv v\cos(\Theta). \tag{B12}$$

Then, since $\mathbf{k}_f\approx\mathbf{k}$, $1\gg\Theta$ and we can replace $\sin(\Theta)\approx\Theta$. Defining

$$\boldsymbol{\eta}\equiv\begin{pmatrix}\eta_x\\ \eta_y\end{pmatrix}\equiv\begin{pmatrix}v\Theta\cos(\alpha)\\ v\Theta\sin(\alpha)\end{pmatrix} \tag{B13}$$

and

$$\boldsymbol{r}_\perp\equiv\begin{pmatrix}x_2\\ y_2\end{pmatrix}, \tag{B14}$$

we can write

$$\int dy_2\int dx_2\int dk_y\int dk_x e^{i(k_xx_2+k_yy_2)}$$
$$\approx\int dy_2\int dx_2\int_0^{2\pi}d\alpha\int_0^\pi d\Theta$$
$$\times\exp[iv\Theta(\cos(\alpha)x_2+\sin(\alpha)y_2)]v^2\Theta$$
$$\approx\int d^2r_\perp\int d^2\eta\,e^{i\boldsymbol{\eta}\cdot\boldsymbol{r}_\perp}, \tag{B15}$$

where we used $v\pi\to\infty$ because $v\gg1$. Integration over $d^2\eta$ then leads to δ distributions in x_2 and y_2, and we finally arrive at

$$I_{fi}^{II}=\left(\frac{2\pi}{L}\right)^{3/2}4\sqrt{2}Z\cos(\gamma)_f k_f^{-4}$$
$$\times\sum\!\!\!\!\!\!\int_a\int_0^\infty dt\langle\phi_f|V_{ee}(\mathbf{r}_1,\mathbf{r}_2=(0,0,vt))|\phi_a\rangle$$
$$\times e^{i(\epsilon_f-\epsilon_a)t}\langle\phi_a|\psi_i(1,\mathbf{r}_2=0)\rangle, \tag{B16}$$

which can then be inserted in Eq. (20) to give Eq. (22).

APPENDIX C: CALCULATION OF HALF-COLLISION INTEGRALS IN MOMENTUM SPACE

In this appendix, we give an example for the calculation of the half-collision integrals in momentum space. We have to deal with integrals of the form

$$I=\int dt\int d^3r\,\phi_f^*(\mathbf{r})\frac{1}{|\mathbf{r}-\mathbf{R}(t)|}\phi_i(\mathbf{r})e^{i\omega t}. \tag{C1}$$

Using Fourier transformations, this can be written in the seemingly more complicated form

$$I=\frac{1}{(2\pi)^6}\int dt\,e^{i\omega t}\int d^3r\int d^3q\int d^3x\frac{e^{i\mathbf{q}\cdot\mathbf{x}}}{|\mathbf{x}|}e^{-i\mathbf{q}\cdot(\mathbf{r}-\mathbf{R})}\int d^3Q\int d^3y\,\phi_f^*(\mathbf{y})\phi_i(\mathbf{y})e^{i\mathbf{Q}\cdot\mathbf{y}}e^{-i\mathbf{Q}\cdot\mathbf{r}}$$
$$=\frac{1}{(2\pi)^6}\int dt\,e^{i\omega t}\int d^3r\int d^3Q\int d^3q\underbrace{\int d^3x\frac{e^{i\mathbf{q}\cdot\mathbf{x}}}{x}}_{\equiv B(\mathbf{q})}\underbrace{\int d^3y\,\phi_f^*(\mathbf{y})\phi_i(\mathbf{y})e^{i\mathbf{Q}\cdot\mathbf{y}}}_{\equiv f(\mathbf{Q})}e^{-i\mathbf{q}(\mathbf{r}-\mathbf{R})}e^{-i\mathbf{Q}\cdot\mathbf{r}}. \tag{C2}$$

Here, $B(\mathbf{q})$ is the Bethe integral

$$B(\mathbf{q})=\frac{4\pi}{q^2}. \tag{C3}$$

We therefore have

$$\begin{aligned} I&=\frac{2}{(2\pi)^5}\int dt\int d^3Q\int d^3q\, e^{i\omega t}\frac{1}{q^2}f(\mathbf{Q})e^{i\mathbf{q}\cdot\mathbf{R}(t)}\\ &\quad\times\int d^3r\, e^{-i(\mathbf{q}+\mathbf{Q})\cdot\mathbf{r}}\\ &=\frac{2}{(2\pi)^2}\int dt\int d^3q\int d^3Q\, e^{i\omega t}\frac{1}{q^2}f(\mathbf{Q})e^{iq_3vt}\delta(\mathbf{q}+\mathbf{Q})\\ &=\frac{2}{(2\pi)^2}\int dt\int d^3q\, e^{i(\omega+q_3v)t}\frac{1}{q^2}f(-\mathbf{q}), \end{aligned} \tag{C4}$$

where in the second step we used $\mathbf{R}(t)=vt\mathbf{e}_z$. With the identity for distributions

$$\int_0^\infty dt\, e^{i\alpha t}=\pi\delta(\alpha)+\mathrm{P}\frac{i}{\alpha}, \tag{C5}$$

Eq. (C4) becomes

$$\begin{aligned} I&=\frac{1}{2\pi}\int_{-\infty}^{\infty}dq_3\int_{-\infty}^{\infty}dq_2\int_{-\infty}^{\infty}dq_1\frac{f(q_1,q_2,q_3)}{(q_1^2+q_2^2+q_3^2)v}\delta\left(\frac{\omega}{v}-q_3\right)\\ &\quad+\frac{i}{2\pi^2}\mathrm{P}\int_{-\infty}^{\infty}dq_3\int_{-\infty}^{\infty}dq_2\int_{-\infty}^{\infty}dq_1\\ &\quad\times\frac{f(q_1,q_2,q_3)}{(q_1^2+q_2^2+q_3^2)(\omega-q_3v)} \end{aligned} \tag{C6}$$

which, of course, helps only if we can evaluate $f(\mathbf{q})$ analytically. To proceed, we make use of the following observations: (a) the final state is a hydrogenic wave function

$$\begin{aligned} \phi_f(\mathbf{r})&=C_l e^{-ikr}k^{l+1}r^l{}_1F_1(l+1-i\eta,2l+2,2ikr)Y_{lm}\\ &=\phi_f(r)Y_{lm} \end{aligned} \tag{C7}$$

and (b) $\phi_i=\phi_i(r)Y_{00}$. Furthermore, we use the expansion

$$e^{i\mathbf{Q}\mathbf{x}}=4\pi\sum_{l'=0}^{\infty}\sum_{m'=-l'}^{l'}i^{l'}j_{l'}(Qx)Y^*_{l'm'}(\hat{\mathbf{Q}})Y_{l'm'}(\hat{\mathbf{x}}). \tag{C8}$$

This leads to

$$\begin{aligned} f(\mathbf{Q})&=\sum_{l'=0}^{\infty}\sum_{m'=-l'}^{l'}\int_0^\infty dr\, r^2\phi_f^*(r)\phi_i(r)\sqrt{4\pi}i^{l'}j_{l'}(Qr)\\ &\quad\times\int d\Omega_{\mathbf{r}}Y^*_{lm}(\hat{\mathbf{r}})Y_{l'm'}(\hat{\mathbf{r}})Y^*_{l'm'}(\hat{\mathbf{Q}})\\ &=\sqrt{4\pi}i^lY^*_{lm}(\hat{\mathbf{Q}})\int_0^\infty dr\,\phi_f^*(r)\phi_i(r)j_l(Qr)r^2. \end{aligned} \tag{C9}$$

We now use

$$j_l(Qr)=\frac{\sqrt{\pi}}{\Gamma(l+3/2)}\left(\frac{1}{4i}\right)^{l+1}\frac{1}{Qr}M_{0,l+1/2}(2iQr) \tag{C10}$$

(where M is Kummer's function) and

$$\begin{aligned} &{}_1F_1(l+1+i\eta,2l+2,-2ikr)\\ &\quad=(-2ikr)^{-(l+1)}e^{-ikr}M_{-i\eta,l+1/2}(-2ikr). \end{aligned} \tag{C11}$$

If we further assume that $\phi_i(r)$ is of the form

$$\phi_i(r)=\sum c_jr^{n_j}e^{-\alpha_j} \tag{C12}$$

with normalization constants c_j and integer n_j (e.g., Roothaan Hartree Fock wave functions [23]), then even the remaining r–integral in Eq. (C9) can be evaluated in a closed form. Using formula (A2) of Ref. [27], we get

$$\begin{aligned} f(\mathbf{Q})&=\sqrt{2\pi k}i^l\frac{|\Gamma(l+1+i\eta)|e^{-\pi/2\eta}}{(2l+1)!\Gamma(l+3/2)}Y^*_{lm}(\hat{\mathbf{Q}})\\ &\quad\times(kQ)^l\sum\frac{c_j\Gamma(2l+3+n_j)}{[\alpha_j+i(Q-k)](2l+3+n_j)}\\ &\quad\times F_2\left(2l+3+n_j,l+1,l+1+i\eta,2l+2,2l\right.\\ &\quad\left.+2;\frac{2iQ}{\alpha_j+i(Q-k)},\frac{-2ik}{\alpha_j+i(Q-k)}\right) \end{aligned} \tag{C13}$$

for continuum final states and

$$\begin{aligned} f(\mathbf{Q})&=i^l\frac{2\pi}{\Gamma(l+3/2)}\sqrt{2}\left(\frac{Z}{n}\right)^{l+3/2}\sqrt{\frac{(n+l)!}{(n-l-1)!2n}}\\ &\quad\times Y^*_{lm}(\hat{\mathbf{Q}})Q^l\sum\frac{c_j\Gamma(2l+3+n_j)}{(\alpha_j+Z/n+iQ)^{(2l+3+n_j)}}\\ &\quad\times F_2\left(2l+3+n_j,l+1,l+1-n,2l+2,2l\right.\\ &\quad\left.+2;\frac{2iQ}{\alpha_j+Z/n+iQ},\frac{2Z/n}{\alpha_j+Z/n+iQ}\right) \end{aligned} \tag{C14}$$

for bound final states, where F_2 is an Appellfunction [28]. After inserting the final expression (C13) into (C6), the angular integrations (over $d\Omega_{\hat{\mathbf{q}}}$) can be carried out analytically again. In the first integral of Eq. (C6), we get

$$\int_{-1}^{1} d(\cos\Theta)\,\delta\left(\frac{\omega}{qv}-\cos\Theta\right)P_l(\cos\Theta) = \begin{cases} P_l\left(\dfrac{\omega}{vq}\right) & \dfrac{\omega}{vq}\in(-1,1) \\ 0 & \text{otherwise,} \end{cases} \tag{C15}$$

and in the principal part integral we can insert the explicit expressions for the P_l, e.g., for $l=0$ we obtain

$$\mathrm{P}\int_{-1}^{1} d(\cos\Theta)\,\frac{P_0(\cos\Theta)}{\omega/vq-\cos\Theta} = \ln\left(\frac{1+\omega/(vq)}{|1-\omega/(vq)|}\right), \tag{C16}$$

where of course the remaining integral over q has to be understood as a principal part integral again. For $l=1,2,3$, we get

$$\mathrm{P}\int_{-1}^{1} d(\cos\Theta)\,\frac{P_1(\cos\Theta)}{\omega/vq-\cos\Theta} = -2+\frac{\omega}{(vq)}\ln\left(\frac{1+\omega/(vq)}{|1-\omega/(vq)|}\right), \tag{C17}$$

$$\mathrm{P}\int_{-1}^{1} d(\cos\Theta)\,\frac{P_2(\cos\Theta)}{\omega/vq-\cos\Theta} = -3\frac{\omega}{(vq)}+\frac{1}{2}\left[3\left(\frac{\omega}{vq}\right)^2-1\right]\ln\left(\frac{1+\omega/(vq)}{|1-\omega/(vq)|}\right), \tag{C18}$$

$$\mathrm{P}\int_{-1}^{1} d(\cos\Theta)\,\frac{P_3(\cos\Theta)}{\omega/vq-\cos\Theta} = \frac{4}{3}-5\left(\frac{\omega}{vq}\right)^2+\frac{1}{2}\frac{\omega}{vq}\left[5\left(\frac{\omega}{vq}\right)^2-3\right]\ln\left(\frac{1+\omega/(vq)}{|1-\omega/(vq)|}\right). \tag{C19}$$

[1] R. Dörner *et al.*, Phys. Rev. Lett. **76**, 2654 (1996).
[2] J.A.R. Samson, Z.X. He, L. Yin, and G.N. Haddad, J. Phys. B **27**, 887 (1994).
[3] K.W. Meyer and C.H. Greene, Phys. Rev. A **50**, R3573 (1994).
[4] J.Z. Tang, S. Watanabe, and M. Matsuzawa, Phys. Rev. A **46**, 2437 (1992).
[5] J.Z. Tang, S. Watanabe, and M. Matsuzawa, Phys. Rev. A **46**, 3758 (1992).
[6] Y. Qiu, J.Z. Tang, J. Burgdörfer, and J. Wang, Phys. Rev. A **57**, R1489 (1998).
[7] A.S. Kheifets and I. Bray, Phys. Rev. A **58**, 4501 (1998).
[8] R. Wehlitz, M.-T. Huang, B.D. DePaola, J.C. Levin, I.A. Sellin, T. Nagata, J.W. Cooper, and Y. Azuma, Phys. Rev. Lett. **81**, 1813 (1998).
[9] R. Wehlitz, T. Pattard, M.-T. Huang, I.A. Sellin, J. Burgdörfer, and Y. Azuma, Phys. Rev. A **61**, 030704(R) (2000).
[10] H.W. van der Hart and C.H. Greene, Phys. Rev. Lett. **81**, 4333 (1998).
[11] J.W. Cooper, Phys. Rev. A **59**, 4825 (1999).
[12] T. Pattard and J. Burgdörfer, Phys. Rev. A **63**, 020701(R) (2001).
[13] J.A.R. Samson, Phys. Rev. Lett. **65**, 2861 (1990).
[14] K. Hino, T. Ishihara, F. Shimizu, N. Toshima, and J.H. McGuire, Phys. Rev. A **48**, 1271 (1993).
[15] J.R. Taylor, *Scattering Theory* (Wiley, New York, 1972).
[16] J.H. Macek and K. Taulbjerg, Phys. Rev. Lett. **46**, 170 (1981).
[17] J.H. Macek and S. Alston, Phys. Rev. A **26**, 250 (1982).
[18] P.K. Kabir and E.E. Salpeter, Phys. Rev. **108**, 1256 (1957).
[19] J.H. McGuire, *Electron Correlation Dynamics in Atomic Collisions* (Cambridge University Press, Cambridge, 1997).
[20] J.H. McGuire, J. Wang, and J. Burgdörfer, Phys. Rev. A **54**, 3668 (1996).
[21] M.R.C. McDowell and J.P. Coleman, *Introduction to the Theory of Ion-Atom Collisions* (North-Holland, New York, 1970).
[22] J.M. Rost and T. Pattard, Phys. Rev. A **55**, R5 (1997).
[23] E. Clementi and C. Roetti, At. Data Nucl. Data Tables **14**, 177 (1974).
[24] F.W. Byron and C.J. Joachain, Phys. Rev. **164**, 164 (1967).
[25] T. Aberg, Phys. Rev. A **2**, 1726 (1970).
[26] A. Dalgarno and H.R. Sadeghpour, Phys. Rev. A **46**, R3591 (1992).
[27] L. Kocbach, J. Phys. B **9**, 2269 (1976).
[28] A. Erdélyi, W. Magnus, F. Oberhettinger, and F.G. Tricomi, *Higher Transcendental Functions* (McGraw–Hill, New York, 1955).